nature geoscience
SUPPLEMENTARY INFORMATION
DOI: 10.1038/NGEO1426

Supplementary information for "A Mantle-Driven Surge in Magma Supply to Kīlauea Volcano During 2003–2007"

This supplement contains information on data collection methods, magma supply estimates for Kīlauea, deformation results from Mauna Loa and Kīlauea's south flank, and deformation modeling procedures and results.

METHODS

All data were collected by staff of the Hawaiian Volcano Observatory (HVO). Processing and analysis methods are detailed below.

Gas emissions

SO_2 emission rate data are collected with an ultraviolet spectrometer (COSPEC or FLYSPEC) during repeated vehicle-based transects beneath gas plumes from Kīlauea's summit and east rift zone (ERZ). Persistent trade winds from the northeast blow the plumes across roads 1 km and 9 km from the summit and ERZ source vents, respectively. Average transect values are combined with wind-speed data to derive emission rates, and error is calculated as the standard deviation of repeated transects. Procedures are given in [refs. 50–52].

CO_2 emissions are constrained using the SO_2 emission rate E_{SO2} and synchronously quantified volcanic CO_2-to-SO_2 molar ratio CO_2/SO_2 measured across the summit plume. The emission rate of CO_2 in tonnes per day is computed as $0.69 \times (CO_2)/(SO_2)\ E_{SO2}$. Methodology is described in [ref. 34].

SO_2 emission rates from the ERZ can be used to assess the volume of magma that has degassed, which indicates the volume of magma that has been transported from the summit to the

ERZ. This calculation, based on knowledge of the CO_2/SO_2 molar ratio from eruptive gas samples from the ERZ, indicates that 1.49 kg of SO_2 is emitted per tonne of lava degassed[36].

Petrology

Samples of eruptive products, collected throughout the ongoing Pu‘u ‘Ō‘ō-Kupaianaha eruption, generally consist of rapidly quenched near-vent tephra and spatter, and lava collected from surface flows, ponds, and tubes (through skylights). Bulk lava major-element analyses (including MgO wt. %) are obtained by wavelength dispersive x-ray fluorescence. Procedures are detailed in [refs. 28,53]. Eruption temperatures are based on geothermometry of MgO glass contents[54]. MgO content and glass temperatures generally track one another, but a noteworthy exception is the time period immediately following the June 19, 2007 ERZ eruption, when samples collected from Pu‘u ‘Ō‘ō had some of the coolest glass temperatures during the 2000–2009 time period. This is most likely caused by a combination of two factors: 1) the samples were spatter, which tend to have lower glass temperatures than quenched molten lava, and 2) the lava erupted within Pu‘u ‘Ō‘ō during the July 1–21, 2007, time period of lowest glass temperatures had clearly been resident beneath Pu‘u ‘Ō‘ō (based on the low gas emissions) and was therefore cooler than if it had been transported from the summit more recently.

Seismicity

Earthquake locations were determined from data collected by seismometers of HVO’s permanent network. The seismic network, data processing, and location procedures are described in [ref. 55].

Deformation

GPS data are collected by a network of continuous instruments, as well as annual (or as activity warrants) surveys of fixed benchmarks. Dual-frequency GPS data are processed using the GIPSY/OASIS II software[56] with non-fiducial orbits and a precise point positioning strategy[57]. A complete description of the GPS network and processing strategy are in [ref. 58].

The distance between GPS stations AHUP and UWEV includes a small amount of tectonic motion (a few cm/yr) because station AHUP moves seaward with the south flank[18,19]; however, this motion is minor compared to extension and contraction due to inflation and deflation of subsurface magma reservoirs during the 2003–2007 magma supply surge.

Leveling data (Fig. 4b) give elevation changes of fixed benchmarks over time. Procedures are described in [ref. 12].

Campaign GPS and leveling data indicate subsidence of benchmark HVO7 (Fig. 4b), about 50 km from Kīlauea's summit along the ERZ (Fig. 1), since the mid-1970s. The subsidence rate at this site is not a function of geothermal production at a power plant ~6.5 km to the west. The power plant came on line in 1993, and no change in the subsidence rate is apparent on or around this time, and power production has been steady. From late 2003 to mid-2007 a stalling of the subsidence is suggested by the GPS and leveling data. The coincidence of the apparent stalling of subsidence and the 2003–2007 increase in magma supply suggests that some magma may have been stored within the lower ERZ during the magma supply surge.

InSAR data are from the ASAR instrument on the ENVISAT satellite, operated by the European Space Agency, and RADARSAT-1, operated by the Canadian Space Agency. Data are processed using the GAMMA software, and topographic phase is corrected using a 30-m-resolution digital elevation model derived from the Shuttle Radar Topography Mission[59].

Coherence in resulting interferograms is improved using an adaptive filtering technique[60], and unwrapping is done using a minimum-cost approach[61].

DEFORMATION MODELING

We modeled deformation data to infer the geometry of magma sources beneath the summit and upper southwest rift zone of Kīlauea Volcano. Modeling was restricted to radar interferometry data, which offers the best spatial resolution of any technique (only 3 GPS stations were present in the summit area in 2006, so adding GPS would not significantly impact the model result). The interferogram selected for modeling is from ENVISAT beam mode 6, track 179, and spans 11 December 2005 to 31 December 2006. Data were inverted to determine the best-fitting point source[62], approximating a magma reservoir, and horizontal uniform-opening rectangular dislocation[63], approximating a sill, in an elastic, isotropic half-space. The best-fitting model (supplementary fig. 1) includes a point source 2.9 km beneath the south caldera, with a volume increase of about 0.009 km^3, and a 4.8 km x 1.2 km sill at 3.8-km depth beneath the upper SWRZ, with an opening of 0.65 m (equivalent to a volume of about 0.004 km^3). The total modeled volume increase during 2006 is therefore about 0.013 km^3.

Our modeling results are approximate for several reasons. Perhaps most importantly, we treat the magma as an incompressible fluid, which may result in an underestimate in volume change by as much as a factor of 5[37,38]. Other factors that can result in different depth and volume change estimates include model geometry (for example, an ellipsoid instead of a point source)[64,65], layering or the presence of weak materials[66,67], non-elastic rheologies[68,69], and degassing and gas ascent[70]. While important to a few factors, the effects of such variables on the

calculated magma supply are of second order, since the volume of extrusion is an order of magnitude larger than the volume of storage beneath the summit and SWRZ.

DEFORMATION OF KĪLAUEA'S SOUTH FLANK

Deformation data indicate opening of Kīlauea's deep rift system between about 3-km and 10-km depth, possibly due to magma accumulation coupled with seaward sliding of the volcano's south flank along a low-angle detachment fault[17–19,71]. During 2003–2008, the rate of south flank motion remained constant (supplementary fig. 2), suggesting that magma was neither stored nor withdrawn from the deep rift zone.

DEFORMATION OF MAUNA LOA

After several years of deflation, GPS results indicated inflation of Mauna Loa volcano, starting in mid-2002[31]. The inflation rate decreased, but remained steady, from late 2002 through early 2004, increased several-fold during mid-2004 to mid-2005, waned, and changed to deflation in late 2009 (supplementary fig. 3). The time period of inflation at Mauna Loa bookends the inflation at Kīlauea, *i.e.*, the magma supply increase that affected Kīlauea was also manifested at Mauna Loa. The two volcanoes erupt isotopically distinct magmas, indicating distinct mantle sources[47], but a surge from the hotspot that feeds both volcanoes could travel through different regions of the mantle before reaching the surface.

PREVIOUS ESTIMATES OF MAGMA SUPPLY TO KĪLAUEA

Since the first estimate of the contemporary magma supply rate to Kīlauea Volcano was published by Swanson[7], many authors have quantified magma supply to Kīlauea over various

time periods, using different techniques. Table S1 details a selection of estimates made for magma supply to Kīlauea's shallow magmatic system (*i.e.*, magma erupted or stored in the summit and shallow rift zones). Magma supply estimates that include the deep rift zones[25] are not included; whether or not magma accumulates in this area of the volcano is uncertain, and no evidence for a change in deep rift opening was found in the current study.

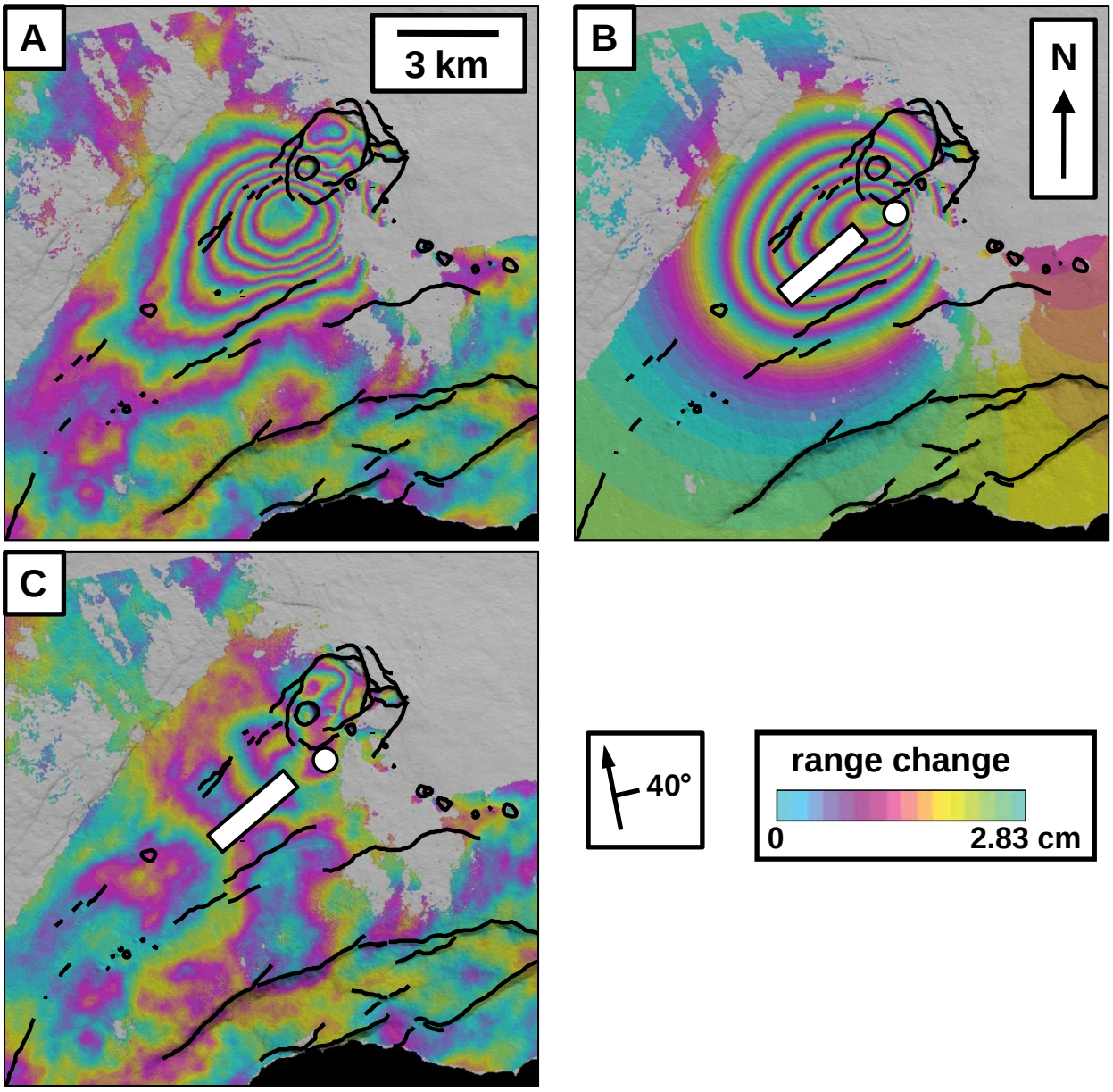

Supplementary Figure 1. Model of deformation during 2006. **a**, Line-of-sight displacements (scale bar at lower right) recorded by an ENVISAT radar interferogram (with azimuth direction to the north-northwest and an incidence angle of 40°, as indicated by the legend) spanning 15 December 2005 to 31 December 2006. **b**, Displacements predicted by a model that includes a point source[62] (white circle) beneath the south caldera at a depth of 2.9 km that expanded by

0.009 km^3, and a rectangular sill[63] (white rectangle) beneath the upper SWRZ, with dimensions of 4.8 km x 1.2 km at a depth of 3.8 km, that opened by about 0.65 m (for a volume increase of 0.004 km^3). Total volume increase in both model sources is 0.013 km^3. **c,** Residual displacements (observed minus modeled) are relatively small compared to the size of the observed signal, demonstrating that the model accounts for most of the deformation. The residual signal probably does not imply a large difference from the modeled volume change given uncertainties inherent in the modeling (see text for discussion).

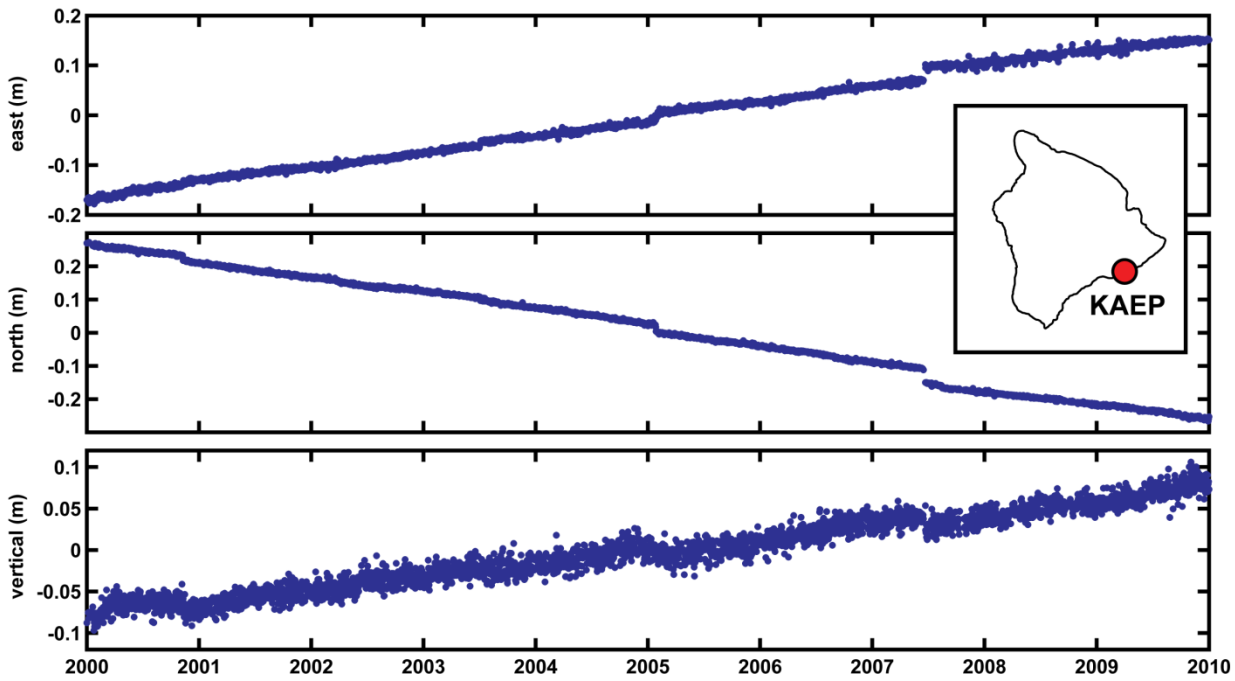

Supplementary Figure 2. Deformation of Kīlauea's south flank. East (top), north (middle), and vertical (bottom) components of deformation at GPS station KAEP, which is located on the south flank of Kīlauea Volcano (location given in inset). Linear deformation suggests no change in the opening rate of the deep rift zone during 2000–2009. Small offsets in the time series are related to aseismic slip events on the south flank[20,21].

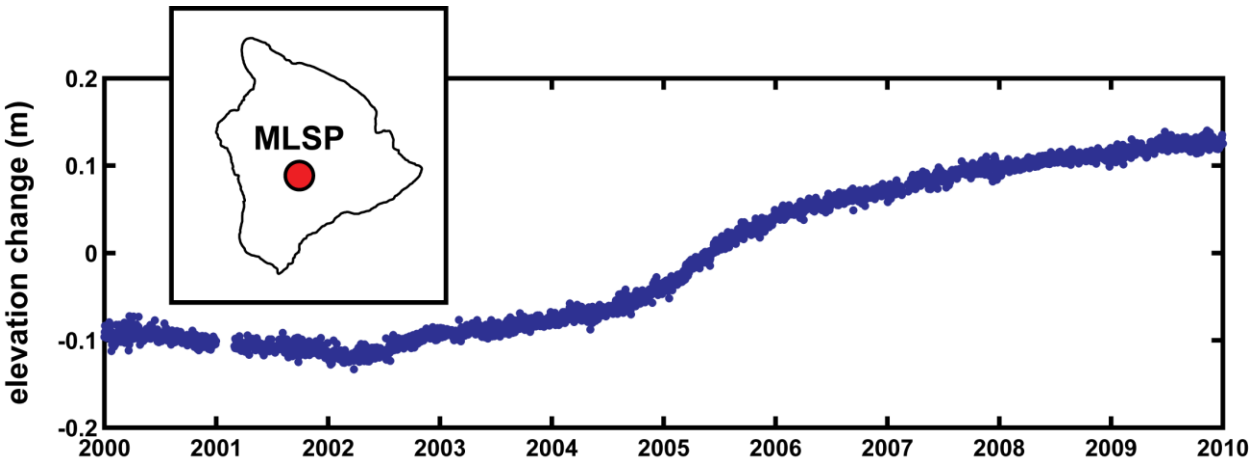

Supplementary Figure 3. Deformation of Mauna Loa. Vertical elevation change at a GPS station MLSP, located on the south side of Mauna Loa's summit caldera (location given in inset). Uplift and inflation began in 2002, accelerated in 2004–2005, and gradually waned to no deformation by the end of 2009[31,45].

Time period	Supply (km^3/yr)	Method	Reference
1918–1979	0.08	Ratio between repose times and erupted volumes	48
1919–1990	0.09	Effusion rate of several sustained eruptions	1
1952–1971	0.11	Effusion rate of three sustained eruptions	7
1956–1983	0.09	Average summit and rift deformation and eruption volumes	24
1959–1990	0.06	Average based on deformation and eruption volumes	1
1960–1967	0.02–0.18	Deformation-inferred refilling of summit reservoir	1
1966–1970	0.07	Deformation and eruption volumes	72
1967-1975	0.05–0.18	Deformation and eruption volumes	73
1971–1972	0.08	Deformation and erupted volumes	32
1975–1977	0.07–0.16	Microgravity and deformation	74
1975-1982	0.08	Deformation and erupted volumes	75
1983–1984	0.12	First 20 episodes of Pu`u `O`o eruption	76
1983–2002	0.12	Pu`u `O`o eruption volumes	26
1983–2002	0.13	SO_2 emissions from ERZ	36
1991	0.08	Deformation and effusion rates	77

Table S1. Magma supply rates to the shallow magma system of Kīlauea Volcano, as determined by previous studies. Estimates that include deep rift opening, for example, [ref. 25]. Calculated supply, time period over which the calculation was made, data used to determine supply, and reference number are given.

References

50. Sutton, A. J., Elias, T., Gerlach, T. M. & Stokes, J. B. Implications for eruptive processes as indicated by sulfur dioxide emissions from Kilauea Volcano, Hawai‘i, 1979–1997. *J. Volcanol. Geotherm. Res.* **108**, 283–302 (2001).

51. Elias, T. *et al.* Comparison of COSPEC and two miniature ultraviolet spectrometer systems for SO2 measurements using scattered sunlight. *Bull. Volcanol.* **68**, 313–322 (2006).

52. Elias, T. & Sutton, A. J. Sulfur dioxide emission rates from Kīlauea Volcano, Hawai‘i, an update; 2002-2006. *U.S. Geol. Surv. Open-File Rep.* **2007–1114** (2007).

53. Thornber, C. R. Olivine-liquid relations of lava erupted by Kilauea Volcano from 1994 to 1998; implications for shallow magmatic processes associated with the ongoing east-rift-zone eruption. *Can. Mineral.* **39**, 239–266 (2001).

54. Helz, R. T. & Thornber, C. R. Geothermometry of Kilauea Iki lava lake, Hawaii. *Bull. Volcanol.* **49**, 651–668 (1987).

55. Nakata, J. N. & Okubo, P. G. Hawaiian Volcano Observatory seismic data, January to December 2008. *U.S. Geol. Sur. Open-File Rep.* **2009–1251** (2009).

56. Lichten, S. & Border, J. Strategies for high-precision Global Positioning System orbit determination. *J. Geophys. Res.* **92**, 12,751–12,762 (1987).

57. Zumberge, J. F., Heflin, M. B., Jefferson, D. C., Watkins, M. M. & Webb, F. H. Precise point positioning for the efficient and robust analysis of GPS data from large networks. *J. Geophys. Res.* **102**, 5005–5017 (1997).

58. Miklius, A. *et al.* Global Positioning System Measurements on the Island of Hawai`i; 1997 through 2004. *U.S. Geol. Surv. Open-File Rep.* **2005–1425** (2005).

59. Farr, T. G. & Kobrick, M. Shuttle Radar Topography Mission produces a wealth of data. *Eos Trans. Am. Geophys. Union* **81**, 583, 585 (2000).

60. Goldstein, R. M. & Werner, C. L. Radar interferogram filtering for geophysical applications. *Geophys. Res. Lett.* **25**, 4035–4038 (1998).

61. Chen, C. W. & Zebker, H. A. Two-dimensional phase unwrapping with use of statistical models for cost functions in nonlinear optimization. *Opt. Soc. Am. A* **18**, 338–351 (2001).

62. Mogi, K. Relations between the eruptions of various volcanoes and the deformations of the ground surfaces around them. *Bull. Earthquake Res. Inst.* **36**, 99–134 (1958).

63. Okada, Y. Surface deformation due to shear and tensile faults in a half-space. *Bull. Seismol. Soc. Am.* **75**, 1135–1154 (1985).

64. Fialko, Y., Khazan, Y. & Simons, M. Deformation due to a pressurized horizontal circular crack in an elastic half-space, with application to volcano geodesy. *Geophys. J. Int.* **146**, 181-190 (2001).

65. Dieterich, J. H. & Decker, R. W. Finite element modeling of surface deformation associated with volcanism. *J. Geophys. Res.* **80**, 4094-4102 (1975).

66. Masterlark, T. Magma intrusion and deformation predictions: Sensitivities to the Mogi assumptions. *J. Geophys. Res.* **112**, B06419 (2007).

67. Crescentini, L. & Amoruso, A. Effects of crustal layering on the inversion of deformation and gravity data in volcanic areas: An application to the Campi Flegrei caldera, Italy. *Geophys. Res. Lett.* **34**, L09303 (2007).

68. Masterlark, T., Haney, M., Dickinson, H., Fournier, T. & Searcy, C. Rheologic and structural controls on the deformation of Okmok volcano, Alaska: FEMs, InSAR, and ambient noise tomography. *J. Geophys. Res.***115**, B02409 (2010).

69. Newman, A. V., Dixon, T. H., Ofoegbu, G. I. & Dixon, J. E. Geodetic and seismic constraints on recent activity at Long Valley Caldera, California: Evidence for viscoelastic rheology. *J. Volcanol. Geotherm. Res.* **105**, 183-206 (2001).

70. Chouet, B. A., Dawson, P. B., James, M. R. & Lane, S.J. Seismic source mechanism of degassing bursts at Kilauea Volcano, Hawaii: Results from waveform inversion in the 10–50 s band. *J. Geophys. Res.* **115**, B09311 (2010).

71. Clague, D. A. & Denlinger, R. P. Role of olivine cumulates in destabilizing the flanks of Hawaiian volcanoes. *Bull. Volcanol.* **56**, 425–434 (1994).

72. Dvorak, J., Okamura, A. & Dieterich, J. H. Analysis of surface deformation data, Kilauea Volcano, Hawaii October 1966 to September 1970. *J. Geophys. Res.* **88**, 9295–9304 (1983).

73. Wright, T. L. & Klein, F. W. in *Dynamics of Crustal Magma Transfer, Storage, and Differentiation*, C. Annen, G. F. Zellmer, Eds. (*Geol. Soc. Spec. Pub.* **304**), Dynamics of magma supply to Kilauea Volcano, Hawaii: integrating seismic, geodetic, and eruption data, 83-116 (2008).

74. Dzurisin D., Anderson, L. A., Eaton, G. P., Koyanagi, R. Y., Lipman, P. W., Lockwood, J. P., Okamura, R. T., Puniwai, G. S., Sako, M. K. & Yamashita, K.M.

Geophysical observations of Kilauea Volcano, Hawaii, 2. Constraints on the magma supply during November 1975-September 1977. *J. Volcanol. Geotherm. Res.* **7**, 241–269 (1980).

75. Johnson, D. J. Molten core model for Hawaiian rift zones. *J. Volcanol. Geotherm. Res.* **66**, 27–35 (1995).

76. Wolfe, E. W., Garcia, M. O., Jackson, D. B., Koyanagi, R. Y., Neal, C. A. & Okamura, A. T. in *Volcanism in Hawaii*, R. W. Decker, T. L. Wright, P. H. Stauffer, Eds. (*U.S. Geol. Surv. Prof. Pap.* **1350**), The Puu Oo eruption of Kilauea Volcano, episodes 1-20, January 3, 1983, to June 8, 1984, 471–508 (1987).

77. Denlinger, R. P. A dynamic balance between magma supply and eruption rate at Kilauea volcano, Hawaii. *J. Geophys. Res.* **102**, 18,091–18,100 (1997).